Quadrupole-driven non-Fermi-liquid and magnetic-field-induced heavy fermion states in a non-Kramers doublet system

T. Onimaru,[1,*] K. Izawa,[2] K. T. Matsumoto,[1] T. Yoshida,[2] Y. Machida,[2] T. Ikeura,[2] K. Wakiya,[1] K. Umeo,[3] S. Kittaka,[4] K. Araki,[5] T. Sakakibara,[4] and T. Takabatake[1,6]

[1]*Department of Quantum Matter, Graduate School of Advanced Sciences of Matter, Hiroshima University, Higashi-Hiroshima 739-8530, Japan*

[2]*Department of Condensed Matter Physics, Graduate School of Science and Engineering, Tokyo Institute of Technology, Tokyo 152-8551, Japan*

[3]*Cryogenics and Instrumental Analysis Division, N-BARD, Hiroshima University, Higashi-Hiroshima 739-8526, Japan*

[4]*Institute for Solid State Physics, University of Tokyo, Kashiwa 277-8581, Japan*

[5]*Department of Applied Physics, National Defense Academy, Yokosuka 239-8686, Japan*

[6]*Institute for Advanced Materials Research, Hiroshima University, Higashi-Hiroshima 739-8530, Japan*

(Received 6 December 2015; revised manuscript received 30 June 2016; published 16 August 2016)

Orbital degrees of freedom in condensed matter could play important roles in forming a variety of exotic electronic states by interacting with conduction electrons. In $4f$-electron systems, because of strong intra-atomic spin-orbit coupling, an orbitally degenerate state inherently carries quadrupolar degrees of freedom. The present work has focused on a purely quadrupole-active system $PrIr_2Zn_{20}$ showing superconductivity in the presence of an antiferroquadrupole order at $T_Q = 0.11$ K. We observed non-Fermi-liquid (NFL) behaviors emerging in the electrical resistivity ρ and the $4f$ contribution to the specific heat, C_{4f}, in the paramagnetic state at $T > T_Q$. Moreover, in magnetic fields $B \leqslant 6$ T, all data sets of $\rho(T)$ and $C_{4f}(T)$ are well scaled with characteristic temperatures T_0's. This observation of the NFL state in the nonmagnetic quadrupole-active system has an origin intrinsically different from that observed in the vicinity of the conventional quantum critical point. It implies possible formation of a quadrupole Kondo lattice resulting from hybridization between the quadrupoles and the conduction electrons with an energy scale of $k_B T_0$. At $T \leqslant 0.13$ K, $\rho(T)$ and $C_{4f}(T)$ exhibit anomalies as B approaches 5 T. This is the manifestation of a field-induced crossover toward a Fermi-liquid ground state in the quadrupole Kondo lattice.

DOI: 10.1103/PhysRevB.94.075134

I. INTRODUCTION

In metals and alloys, localized d and/or f electrons inherently possessing "spin" and "orbital" degrees of freedom are dominant sources of not only various magnetic phenomena but also unconventional superconductivity. Extensive studies on a lot of spin-active systems have successfully revealed the variety of the magnetic phenomena arising from competition of the intersite Ruderman-Kittel-Kasuya-Yosida (RKKY) interaction and the on-site magnetic Kondo effect, which was represented as the well-known "Doniach diagram" [1]. On the other hand, there is less variety of research on orbital-driven physics. Although the orbital itself must have potential variety, there is little evidence of interplay between the orbital degrees of freedom and the conduction electron.

In the f-electron systems, strong intra-atomic spin-orbit coupling forces the spin and orbital degrees of freedom to be described in terms of the total angular momentum $\boldsymbol{J}$. When the magnetic moment due to $\boldsymbol{J}$ interacts strongly with itinerant conduction electrons, physically observable quantities follow the Fermi-liquid (FL) model of Landau, which is known as a heavy fermion state. When some conditions are fulfilled unexpectedly, the FL state could become unstable; instead, an anomalous metallic state would emerge, a so-called non-Fermi-liquid (NFL) state [2–5]. In the vicinity of the quantum critical point, there emerges unconventional superconductivity [6].

On the other hand, the emergence of a different type of NFL state was theoretically predicted, in the case that electric quadrupoles of the localized f electrons, which become active only in an orbitally degenerate state, interact with the conduction electrons, that is the quadrupole (two-channel) Kondo effect [7]. It is quite different from the ordinary (single-channel) *magnetic* Kondo effect in terms of the scattering process of the conduction electrons; the scattering source is not magnetic dipole but the time-reversal electric quadrupole. Thereby, the impurity quadrupoles were overcompensated by the conduction electrons, leading to the residual entropy of $(0.5)R\ln 2$ and the NFL behavior: the magnetic susceptibility χ and the specific heat divided by temperature, C/T, show $\ln T$ dependence, and the electrical resistivity follows $\rho - \rho_0 \propto 1 + A\sqrt{T}$, where ρ_0 is residual resistivity and A is a coefficient [7,8]. The NFL state and the residual entropy were also expected in a quadrupole Kondo "lattice," in which quadrupole moments are periodically placed [9]. Very recently, the peculiar temperature dependence of $\rho(T)$ and $C(T)$ have been theoretically predicted as described later [10,11]. Moreover, in the lattice model, different types of electronic ordered states have been proposed [12–14]. Nevertheless, there is no experimental evidence on the exotic states, probably because there are rare systems carrying purely active quadrupoles.

Over the past few decades, experimental efforts have addressed the issues that could arise from the impurity quadrupole Kondo effect [15]. NFL behaviors were observed in uranium- and praseodymium-based systems with $5f^2$ and $4f^2$ configurations, respectively, such as $U_xY_{1-x}Pd_3$ [16,17],

*onimaru@hiroshima-u.ac.jp

UBe_{13} [18], $U_xTh_{1-x}Be_{13}$ [19], $U_xTh_{1-x}Ru_2Si_2$ [20], and $Pr_xLa_{1-x}Pb_3$ [21]. However, there is no firm experimental evidence for the impurity quadrupole Kondo effect, since atomic disorder or uncertainty in the crystalline electric-field (CEF) ground states particularly in the U-based systems prevent the clarification.

Recently, a family of the praseodymium-based systems PrT_2X_{20} (T: transition metals, X: Al, Zn, and Cd) have emerged as a prototype to study the quadrupole Kondo effect, since the CEF ground state is a non-Kramers doubly degenerated state, that is labeled as the Γ_3 doublet in the cubic T_d point group, having no magnetic dipoles but electric quadrupoles [22–27]. In $PrIr_2Zn_{20}$, an antiferroquadrupolar (AFQ) order occurs at $T_Q = 0.11$ K [23]. Although the entropy release of $R\ln 2$ is expected from an order of the doubly degenerated CEF ground state, the entropy at T_Q estimated from the specific heat is only 20% of $R\ln 2$. Therefore, there should be another mechanism, except the AFQ order, which consumes the rest of the entropy above T_Q. On the other hand, below T_Q, a superconducting transition sets in at $T_c = 0.05$ K, suggesting a possible interplay between the quadrupole fluctuations and the superconducting Cooper-pair formation [23,28–30]. The coexistence of superconductivity with quadrupole order also manifests in isostructural compounds $PrRh_2Zn_{20}$, $PrTi_2Al_{20}$, and PrV_2Al_{20} [31–34]. In $PrTi_2Al_{20}$ and PrV_2Al_{20}, the strong hybridization between the $4f$ elections and the conduction electrons was revealed by the Al-NMR and Pr $3d$–$4f$ resonant photoemission measurements [35,36]. The large Seebeck coefficient divided by temperature S/T observed in PrT_2Al_{20} (T = Ti, V, and Ta) also suggests the strong hybridization effect, although that for $PrIr_2Zn_{20}$ at $B = 0$ is two or three orders smaller than those of PrT_2Al_{20} [37]. In $PrIr_2Zn_{20}$, the cyclotron effective mass m_c less than the bare electron mass m_0 was observed in the de Haas van Alphen measurements [38]. PrV_2Al_{20} exhibits NFL behavior above $T_Q = 0.6$ K; the $4f$ contributions in both ρ and χ follow $\sqrt{T}$ for $2 < T < 20$ K [24], however, in the temperature range, the magnetic degrees of freedom in the first excited state must interfere in the NFL behavior. Quadrupolar quantum criticality induced by application of magnetic field has been proposed [39].

In the present work, we study the transport, thermodynamic, and magnetic properties for the non-Kramers doublet system $PrIr_2Zn_{20}$ in magnetic fields applied along the [100] direction. For B||[100], the AFQ order collapses at around 5 T, whose value is much lower than the critical fields for the AFQ order in the [110] and [111] field directions [23,28,40]. Since high quality of the sample is necessary to reveal the inherent behavior arising from the quadrupolar degrees of freedom as described above, we have chosen single-crystalline samples with low residual resistivity of 0.2 $\mu\Omega$ cm (residual resistivity ratio, RRR > 100) [23]. The manifestation of the AFQ order guarantees the high quality of the crystals, otherwise it is destroyed by the atomic disorder. Our measurements of the specific heat and the electrical resistivity in magnetic fields have revealed emergence of the NFL state possibly arising from formation of a quadrupole Kondo lattice. Furthermore, we have observed a magnetic-field-induced crossover from the NFL state to an exotic heavy fermion ground state in the quadrupole Kondo lattice.

II. EXPERIMENT

Single-crystalline samples of $PrIr_2Zn_{20}$ used in the present work were grown by using the melt-growth method described in the previous papers [30]. Magnetization was measured using a commercial superconducting quantum interference device (SQUID) magnetometer (Quantum Design MPMS) between 1.9 and 350 K in magnetic fields up to 5 T. Magnetization measurements at low temperatures down to 0.045 K were performed by a capacitive Faraday method using a high-resolution capacitive force-sensing device installed in a ^{3}He-^{4}He dilution refrigerator [41]. Electrical resistance was measured by a standard four-probe dc method in a laboratory-built system with a ^{3}He-^{4}He dilution refrigerator. Thermopower was measured using a laboratory-made probe by applying a temperature difference of 0.04–0.3 K along a bar-shaped sample. Specific heat in magnetic fields was measured by a relaxation method at temperatures between 0.4 and 300 K. The measurements at low temperatures down to 0.06 K were done under quasiadiabatic conditions with a ^{3}He-^{4}He dilution refrigerator equipped with a superconducting magnet of 15 T.

III. RESULTS AND DISCUSSION

A. Specific heat

Figure 1(a) shows the temperature dependence of the $4f$ contribution to the specific heat, C_{4f}, of $PrIr_2Zn_{20}$ in magnetic fields $B \leqslant 12$ T applied along the [100] direction. To estimate the $4f$ contribution C_{4f} to the total specific heat C, we subtracted the nuclear and phonon contributions $C_{\rm nuc}$ and $C_{\rm ph}$ as described below. The Hamiltonian of a nuclear spin of a Pr nucleus, $I = 5/2$, in magnetic field $\boldsymbol{B}$ can be represented as

$$\mathcal{H}_{\rm nuc} = A_{\rm hf}\mathbf{J}\cdot\mathbf{B} - g_N\mu_N\mathbf{B}\cdot\mathbf{I}, \quad (1)$$

where $A_{\rm hf} = 0.052$ K is a coupling constant of hyperfine interaction of a Pr ion [42], and $\boldsymbol{J}$, $g_N = 1.72$, and μ_N are the total angular momentum of $4f$ electrons, nuclear g factor, and nuclear magneton, respectively. The component of $\boldsymbol{J}$ along the magnetic-field direction was regarded as the isothermal magnetization measured at $T = 0.045$ K. Thereby, the nuclear specific heat was estimated by taking the eigenvalues of the Hamiltonian into consideration. The nuclear contribution is zero in $B = 0$. Applying magnetic field, it gradually increases on cooling, e.g., in $B = 3$ T, $C_{\rm nuc}$ is increased up to about 3.5 J/K mol at 0.1 K. The contribution of the phonon was subtracted by using the specific heat of the La analog $LaIr_2Zn_{20}$. The main panel of Fig. 1(b) shows the entropy S_{4f} estimated by integrating C_{4f}/T. The value of S_{4f} reaches $R\ln 2$ at 2 K, supporting that the physical properties at $T < 2$ K are governed by the ground-state doublet.

The sharp peak at $T_Q = 0.11$ K for $B = 0$ in Fig. 1(a) is the manifestation of the AFQ order [23,28,29]. As shown with the open triangles in the inset of Fig. 1(b), upon applying magnetic field for $B \geqslant 3$ T, the peak shifts to lower temperatures and disappears at $B = 4.5$ T. The behavior of the specific-heat peak at T_Q in the magnetic fields is much different from the previous report where the peak is split into two for $1 \leqslant B \leqslant 3$ T [23]. This inconsistency results from an extrinsic effect of another grain contained in the previous sample whose crystalline axis is directed away from the a axis of the dominant crystal.

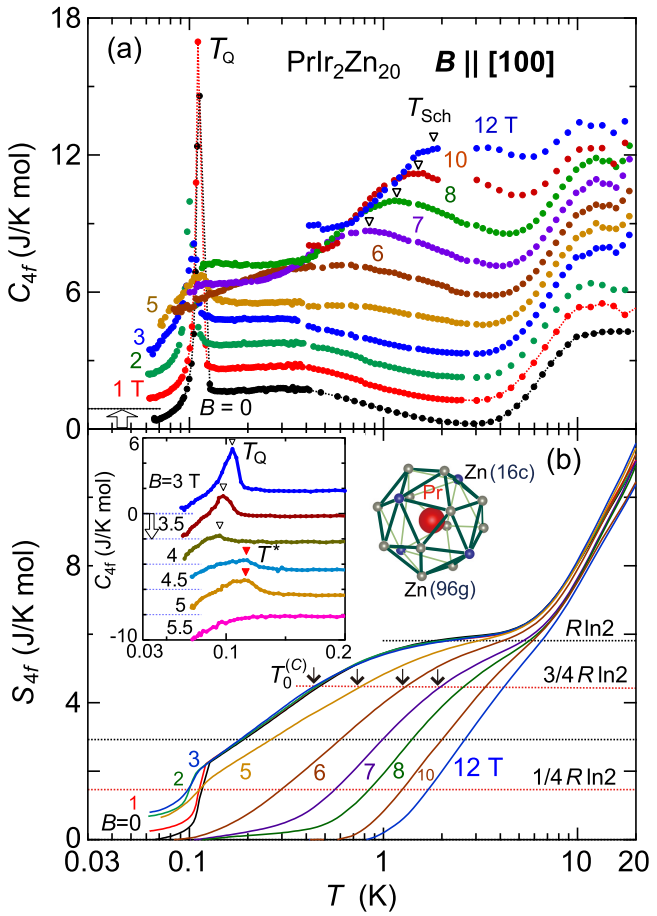

FIG. 1. (a) $4f$ contribution to the specific heat C_{4f} of $PrIr_2Zn_{20}$ in magnetic fields up to 12 T applied along the [100] direction. The data of C_{4f} are vertically offset for clarity. T_Q indicates the temperature of AFQ order. The open triangles are T_{Sch}, where Schottky-type peaks appear as a result of the splitting of the ground-state doublet by applying the magnetic fields. (b) Entropy S_{4f} estimated by integrating $C_{4f}(T)/T$ in various fields. The arrow indicates characteristic temperature $T_0^{(C)}$ defined as the temperature where S_{4f} reaches $\frac{3}{4}R\ln 2$. The inset shows the data of C_{4f} for $3 \leqslant B \leqslant 5.5$ T plotted with vertical offsets. The open and closed triangles, respectively, represent T_Q and a crossover temperature T^* emerging only in $B = 4.5$ and 5 T, which will be described in the text. A Pr ion encapsulated into the symmetric Zn cage, which is formed by four Zn atoms at the 16c site and 12 Zn atoms at the 96g site, is also shown in the inset.

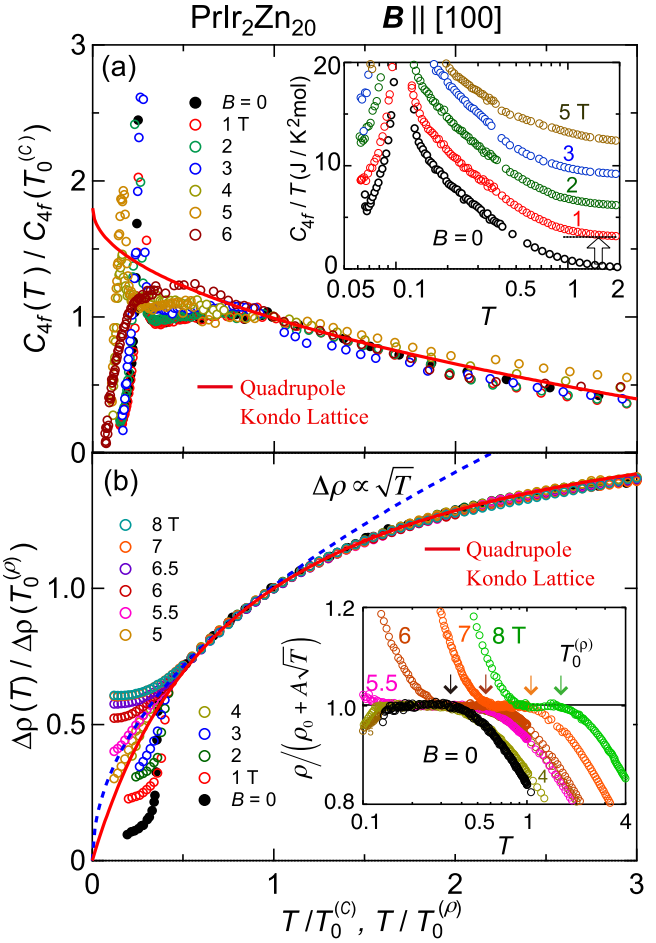

FIG. 2. Scaling plots of (a) the specific heat C_{4f} and (b) the electrical resistivity $\Delta\rho$ of $PrIr_2Zn_{20}$ in the magnetic fields B||[100]. In the temperature region $0.8 < T/T_0^{(C)}, T/T_0^{(\rho)} < 3$, C_{4f}, and $\Delta\rho$ in magnetic fields better follow the calculation by using a two-channel Anderson lattice model [11] as shown with the (red) solid curves than the (blue) dashed curve calculated with the impurity quadrupole Kondo model [7]. The inset of (a) shows the temperature dependence of C_{4f}/T with vertical offsets. The temperature variation of $\rho/(\rho_0+A\sqrt{T})$ is shown in the inset of (b). At the value of 1, $\rho(T)$ follows $\sqrt{T}$. The arrows show the characteristic temperature, $T_0^{(\rho)}$, where $\rho(T)$ deviates from $\rho_0+A\sqrt{T}$ relation.

On the other hand, as shown with the open triangles in Fig. 1(a), $C_{4f}(T)$ in $B = 6$ T shows a broad peak at 0.6 K, which shifts to 2 K with increasing B up to 12 T. The height and width can be explained by taking account of the Zeeman splitting of the ground-state doublet. Because the split singlets lose quadrupolar degrees of freedom, no phase transition occurs in $B > 6$ T.

We pay attention to another broad peak in C_{4f} ($B = 0$) at around 0.4 K in Fig. 1(a). When C_{4f}/T is plotted vs $\ln T$ in the inset of Fig. 2(a), we find the $-\ln T$ dependence between 0.2 and 0.8 K. Since this $-\ln T$ dependence of C_{4f}/T emerges below 2 K, it arises from the degrees of freedom of the Γ_3 ground state. Here, we define a characteristic temperature, $T_0^{(C)}$, as the temperature where S_{4f} reaches $\frac{3}{4}R\ln 2$. This definition follows Cox's definition of the Kondo temperature T_K for the impurity quadrupole Kondo model [7]. As shown in Fig. 1(b), a defined $T_0^{(C)}$ remains at around 0.4 K up to $B = 3$ T and increases for $B > 3$ T [see Fig. 5(a)]. We plot in Fig. 2(a) the values of $C_{4f}(T)/C_{4f}(T_0)$ at various fields, which are well scaled with respect to $T/T_0^{(C)}$ in the range of $T/T_0^{(C)} > 0.8$. This scaling behavior will be discussed in detail by combining the NFL behavior of the electrical resistivity.

B. Electrical resistivity

The temperature dependence of the electrical resistivity $\rho(T)$ in magnetic fields between 0 and 9 T applied along the [100] direction is shown in Fig. 3. It is noted that all the data are plotted without offset. In $B \leqslant 4$ T, $\rho(T)$ shows

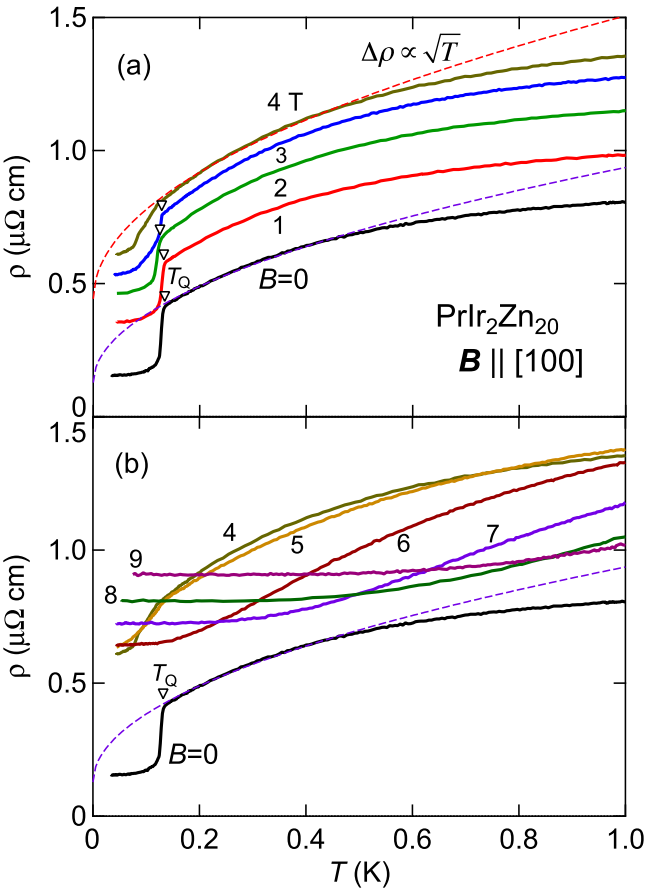

FIG. 3. Temperature dependence of the electrical resistivity of $PrIr_2Zn_{20}$ in magnetic fields of (a) $0 \leqslant B \leqslant 4$ T and (b) $B \geqslant 4$ T applied along the [100] direction. The open triangles indicate the AFQ ordering temperature T_Q. The dashed lines are fits to the data using the relation of $\Delta\rho \propto \sqrt{T}$. It is noted that the data are plotted without offset.

upward convex curvature at $T_Q < T < 1.0$ K, that is the NFL behavior. On cooling below 0.5 K, $\rho(T)$ is likely to follow the $\sqrt{T}$ variation as shown with the dashed lines. The absolute value of $\rho(T)$ for $B \leqslant 4$ T is increased with increasing the magnetic field. On the other hand, as shown in Fig. 3(b), $\rho(T)$ shows downward curvature above 6 T. The residual resistivity is increased with increasing the magnetic field.

We pay our attention to the NFL behavior of the upward convex curve at $T_Q < T < 1.0$ K. The data of $\rho(T)$ are replotted in the inset of Fig. 2(b) as $\rho/(\rho_0 + A\sqrt{T})$ vs T, where ρ_0 is the residual resistivity. In the T region where $\rho/(\rho_0 + A\sqrt{T})$ stays at 1.0, $\Delta\rho = \rho(T) - \rho_0$ follows $\sqrt{T}$. The arrows denote the characteristic temperature, $T_0^{(\rho)}$, where $\rho(T)$ starts deviating from the $\sqrt{T}$ dependence on heating. We represent the data of $\Delta\rho(T)/\Delta\rho(T_0)$ vs $T/T_0^{(\rho)}$ in Fig. 2(b), where $\rho(T)$ follows the scaling well in the temperature range of $0.5 < T/T_0^{(\rho)} \leqslant 3$. As shown in the inset of Fig. 2(b), $T_0^{(\rho)}$ stays at around 0.35 K up to $B = 4$ T, and increases significantly once B exceeds 4 T [see the (red) opened diamonds in Fig. 5(a)]. The field dependence of $T_0^{(\rho)}$ coincides with that of $T_0^{(C)}$ described in the previous subsection, suggesting the same origin of both $T_0^{(\rho)}$ and $T_0^{(C)}$ [15].

C. Non-Fermi-liquid behavior for $T > T_Q$

Let us discuss possible mechanisms for the observed NFL behaviors of $C_{4f}(T)$ and $\Delta\rho(T)$ in the magnetic fields well scaled with respect to $T/T_0^{(C)}$ and $T/T_0^{(\rho)}$, respectively. One is the contribution of a rattling phonon, which gives rise to $\Delta\rho \propto \sqrt{T}$ [43]. There is an optical phonon excitation at around 7 meV (80 K), which is attributed to the low-energy vibration of the Zn atoms surrounding the Pr ion [44–46]. However, as this phonon excitation probably ceases at $T < 1$ K, interaction of the optical-phonon mode with the conduction electrons must be too weak to modify the low-temperature electronic transport.

The second is the impurity quadrupole Kondo effect predicted by Cox *et al.*, which leads to $\Delta\rho(T) \propto 1 + A\sqrt{T}$ and $C/T \propto -\ln T$ as mentioned in the Introduction [7]. The $\sqrt{T}$ dependence of $\rho(T)$ may be applicable to the present data. However, in the present case of $PrIr_2Zn_{20}$, the quadrupole moments are not included as impurities but placed periodically; therefore formation of the quadrupole Kondo lattice is a promising candidate bringing about the NFL state [9]. The theoretical analyses on the temperature variations of ρ and C with the two-channel Anderson lattice model have led to the following relations:

$$\Delta\rho(T) = \frac{a_1}{1 + a_2\left(T_0^{(\rho)}/T\right)}, \tag{2}$$

$$C(T) = b_1\left(1 - b_2\sqrt{\frac{T}{T_0^{(C)}}}\right), \tag{3}$$

where a_i and b_i ($i = 1$ and 2) are parameters [11]. The calculations are shown by the (red) solid curves in Figs. 2(a) and 2(b). The curves are in better agreement with our experimental data for a wider temperature range than those calculated by the impurity quadrupole Kondo model as shown with the (blue) dashed line.

In the present case, the NFL behavior does not persist down to the low-temperature limit. This is certain because this NFL behavior does not arise from the conventional quantum critical point but from the quadrupole Kondo effect. As described in the Introduction, the quadrupoles are overcompensated by the conduction electrons, leading to the unstable electronic state with the residual entropy of $(0.5)R\ln 2$ at zero temperature in principle. In real systems, however, the residual entropy should go to zero at $T = 0$ by a mechanism following the third law of thermodynamics. In fact, in the magnetic fields $B \leqslant 4$ T, the residual entropy is released by the intersite quadrupole interaction, leading to occurrence of the quadrupole order. Thereby, the NFL behavior can manifests itself in the limited temperature range, where the magnetic entropy goes down from $R\ln 2$ to $(0.5)R\ln 2$. In zero magnetic field, the NFL behaviors of the electrical resistivity and the specific heat appear in the temperature range from 1.5 to 0.2 K.

Taking the experimental results and the analyses on them, this is an observation of the NFL state in the nonmagnetic quadrupole-active system, whose origin is intrinsically different from that observed in the vicinity of the conventional quantum critical point. The scaling plots of $C(T)$ and $\Delta\rho(T)$ using the characteristic temperatures $T_0^{(C)}$ and $T_0^{(\rho)}$, respectively, as shown in Figs. 2(a) and 2(b), imply the formation of

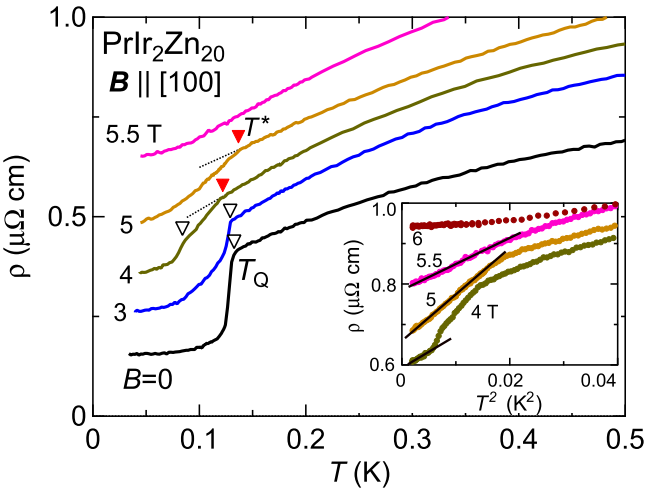

FIG. 4. Temperature dependence of the electrical resistivity $\rho(T)$ of $PrIr_2Zn_{20}$ in the magnetic field of $0 \leqslant B \leqslant 5.5$ T applied along the [100] direction. The data in the magnetic fields are offset for clarity. The open and solid triangles indicate the AFQ order temperature T_Q and the crossover temperature T^*, respectively. The inset is the plot of ρ vs T^2 in $4 \leqslant B \leqslant 6$ T with vertical offset.

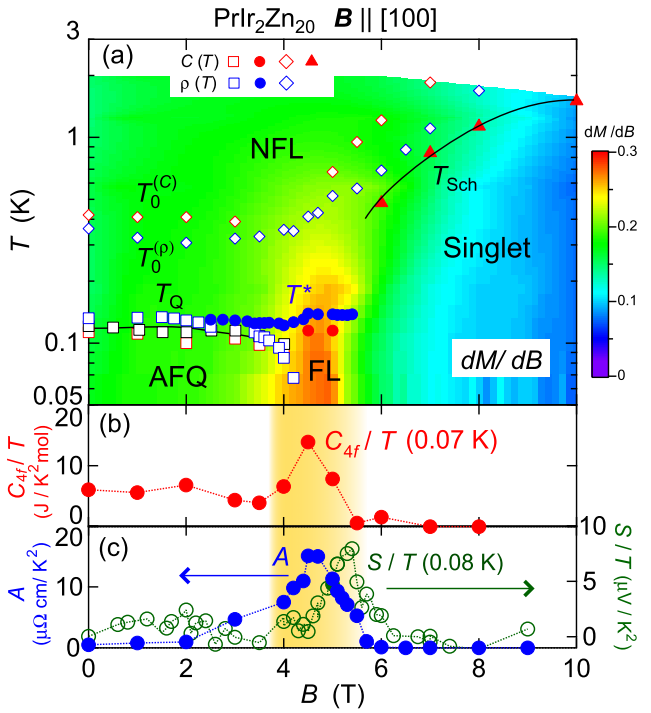

FIG. 5. (a) Magnetic-field vs temperature phase diagram of $PrIr_2Zn_{20}$ for $B||[100]$. The contour plot is made from the derivative of the magnetization with respect to the magnetic field, dM/dB, as shown in Fig. 6(b). The NFL state passes through the region denoted by T^* to the field-induced Fermi-liquid ground state, FL. $T_0^{(C)}$ and $T_0^{(\rho)}$ are the characteristic temperatures for the NFL behavior determined by the measurements of the specific heat and the electrical resistivity, respectively. T_{Sch} is the temperature where a Schottky-type peak appears due to the splitting of the ground-state doublet. (b) Magnetic-field variation of the specific heat divided by temperature, C_{4f}/T at 0.07 K. (c) Coefficient A of the electrical resistivity, $\rho = \rho_0 + AT^2$ (left-hand scale) and the Seebeck coefficient divided by temperature, S/T, at 0.08 K (right-hand scale) [47].

the quadrupole Kondo lattice resulting from the hybridization between the quadrupoles and the conduction electrons with an energy scale of $k_B T_0$.

D. Magnetic-field-induced Fermi-liquid state

Looking closely at the data of $\rho(T)$ at $B = 4$ T, as shown with the solid triangles in Fig. 4, we find another knee at $T^* = 0.12$ K above $T_Q = 0.08$ K. In contrast to the drop of T_Q at $B > 3$ T, T^* stays at around 0.13 K for $B = 4$ and 5 T. As shown in the inset of Fig. 1(b), this T^* coincides with the broad peak of $C_{4f}(T)$ at $T^* = 0.12$ K in $B = 4.5$ and 5 T. The field dependencies of T^* observed in the $\rho(T)$ and $C_{4f}(T)$ measurements are plotted with the blue and red closed circles, respectively, in the B-T phase diagram in Fig. 5(a). The T^* line can be a boundary of two states, meaning a phase transition or a crossover. In the present case, the crossover is likely to occur at T^*, because the peak of $C_{4f}(T)$ becomes very broad despite the rather robust T^* against the magnetic field. On cooling below T^*, $\rho(T)$ follows $\rho_0 + AT^2$ at low temperature for $4 \leqslant B < 6$ T, as shown in the inset of Fig. 4. The A coefficient as a function of B plotted in Fig. 5(c) is strongly enhanced at around 4.5 T.

Figures 6(a) and 6(b) show the isothermal magnetization and the derivative of the magnetization with respect to the magnetic field, dM/dB, at $T = 0.045$, 0.08, 0.17, 0.55, and 1.2 K in the magnetic field of $B \leqslant 14$ T applied along the [100] direction, respectively. The isothermal magnetization shows metamagnetic behavior at around 5 T, where dM/dB shows a peak. The peak shifts slightly to higher fields and becomes broader with increasing temperatures. The contour plot in Fig. 5(a) indicates dM/dB shown in Fig. 6(b). Note that the dM/dB is largely enhanced only in the narrow range of B, $3.5 < B < 5.5$ T, and the peak of dM/dB is likely to be connected to the Schottky anomaly at T_{Sch} due to the splitting of the Γ_3 doublet in the magnetic field for $B \geqslant 6$ T.

Moreover, as shown in Figs. 5(b) and 5(c), there are peaks at 4.5 T in the $4f$ contribution to the specific heat divided by temperature, C_{4f}/T at 0.07 K and the A coefficient of the electrical resistivity. There is also a peak at 5.5 T in the Seebeck coefficient divided by temperature, S/T, at 0.08 K [47]. In addition, it was reported that the elastic modulus of the C_{11} mode, which is a part of the Γ_3-type $(C_{11}–C_{12})/2$ mode, shows strong softening in the magnetic field at around $B = 5$ T [28]. The coincidence of these anomalies at around 5 T suggests development of an exotic Fermi-liquid state on cooling through T^* in a narrow range of B, $3.5 < B < 5.5$ T.

There are some possible mechanisms to form the exotic Fermi-liquid state at $T < T^*$. One is a crossover from the NFL state to a FL state expected in the two-channel Kondo model taking in magnetic-field effect [48]. Perhaps, emergence of a FL state accompanied with a free magnetic spin in the vicinity of the NFL state has been pointed out by taking into account possible competition between the magnetic and quadrupole Kondo effects on the basis of an extended two-channel Kondo model [49]. Another is a crossover due to the composite electronic order [12,13] or the Hastatic order [14] in the quadrupole Kondo lattice. In any case, it is noted that the

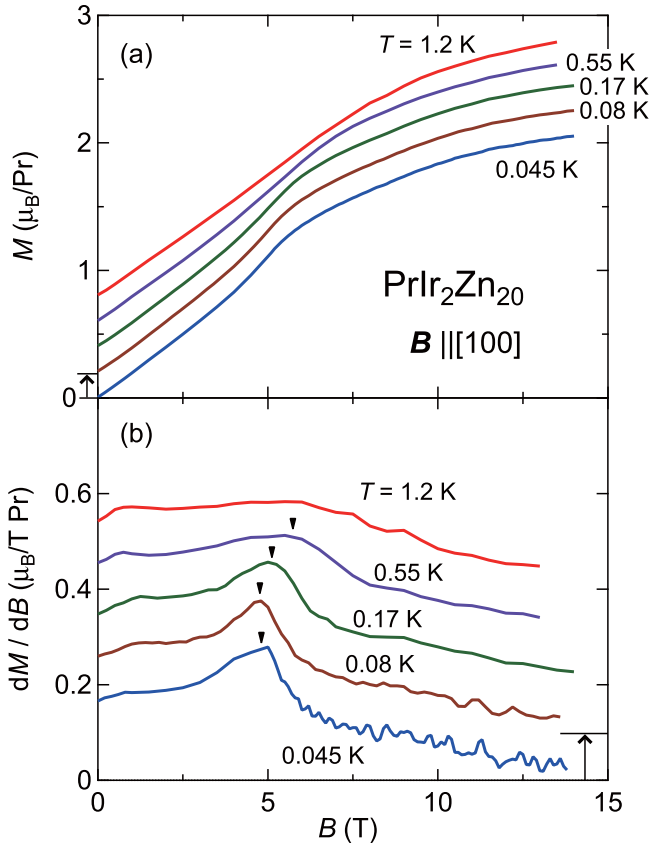

FIG. 6. (a) Isothermal magnetization and (b) dM/dB of $PrIr_2Zn_{20}$ at temperatures between 0.045 and 1.2 K in the magnetic field $B \leqslant 14$ T applied along the [100] direction. The data are vertically offset for clarity.

hybridization between the quadrupoles and the conduction electrons gives rise to a different type of electronic ground state. It is highly desirable to detect the order parameter by microscopic techniques.

Indeed, we expected that the quadrupole-induced quantum critical behavior in $C_{4f}(T)$ would appear when the AFQ order is fully suppressed. However, as shown in Fig. 5(b), C_{4f}/T does not diverge in the vicinity of 4.5 T on cooling to 0.07 K at all. It seems that the Doniach picture is not valid for this pure quadrupole system. Although it is still an open question why the quantum criticality was not detected in $PrIr_2Zn_{20}$, a peculiar feature of the quadrupole must give rise to the unique electronic phenomena.

IV. SUMMARY

We report the low-temperature transport, thermodynamic, and magnetic properties on a cubic system $PrIr_2Zn_{20}$ in which the non-Kramers doublet ground state has purely the quadrupolar degrees of freedom. In the moderately wide temperature range at $T > T_Q$, non-Fermi-liquid behaviors were clearly observed in the electrical resistivity ρ and the specific heat C_{4f}. Both ρ and C_{4f} in magnetic fields $B < 6$ T applied along the [100] direction can be well scaled with characteristic temperatures T_0's, suggesting the formation of the quadrupole Kondo lattice due to the hybridization between the quadrupoles and the conduction electrons. It indicates that the NFL behavior observed in the present system is intrinsically different from that observed in the vicinity of the conventional quantum critical point. Furthermore, ρ and C_{4f} exhibit anomalies at $T^* = 0.13$ K in the vicinity of 5 T, where the coefficient A for $\rho = \rho_0 + AT^2$, C_{4f}/T, and S/T, have significant enhancement as a function of B. The concomitant increase in dM/dB indicates formation of a magnetic-field-induced Fermi-liquid ground state to remove the residual entropy in the quadrupole Kondo lattice. These observations imply that the Doniach picture relevant to the spin Kondo systems should not be valid for this purely quadrupole-active system, possibly leading us beyond the Doniach picture.

ACKNOWLEDGMENTS

The authors would like to thank A. Tsuruta, K. Miyake, H. Kusunose, S. Hoshino, J. Otsuki, Y. Kuramoto, Y. Sugano, K. Uenishi, Y. Yamane, I. Ishii, T. Suzuki, K. Matsubayashi, and K. Iwasa for helpful discussions. We also thank Y. Shibata for the electron-probe microanalysis performed at N-BARD, Hiroshima University. The magnetization measurements with MPMS and specific-heat measurements with PPMS were carried out at N-BARD, Hiroshima University. This work was financially supported by JSPS KAKENHI Grants No. 21102516, No. 23102718, No. 26707017, No. 15K05158, No. 15H05883, No. 15H05884, and No. 15H05886 (J-Physics), and by The Mazda Foundation Research Grant, Japan and Hiroshima University Fujii Research Fund.

[1] J. Flouquet, On the heavy Fermion road, Prog. Low Temp. Phys. **15**, 139 (2005).

[2] H. v. Löhneysen, A. Rosch, M. Vojta, and P. Wolfle, Fermi-liquid instabilities at magnetic quantum phase transitions, Rev. Mod. Phys. **79**, 1015 (2007).

[3] K. Umeo, H. Kadomatsu, and T. Takabatake, Non-Fermi- liquid behaviour at the pressure-induced antiferromagnetic to nonmagnetic transition in a heavy-fermion compound, Ce_7Ni_3, J. Phys.: Condens. Matter **8**, 9743 (1996).

[4] J. Custers, P. Gegenwart, H. Wilhelm, K. Neumaier, Y. Tokiwa, O. Trovarelli, C. Geibel, F. Steglich, C. Pépin, and P. Coleman, The break-up of heavy electrons at a quantum critical point, Nature (London) **424**, 524 (2003).

[5] Q. Si, S. Rabello, K. Ingersent, and J. L. Smith, Locally critical quantum phase transitions in strongly correlated metals, Nature (London) **413**, 804 (2001).

[6] N. D. Mathur, F. M. Grosche, S. R. Julian, I. R. Walker, D. M. Freye, R. K. W. Haselwimmer, and G. G. Lonzarich, Magnetically mediated superconductivity in heavy fermion compounds, Nature (London) **394**, 39 (1998).

[7] D. L. Cox and Z. Zawadowski, Exotic Kondo effects in metals: Magnetic ions in a crystalline electric field and tunneling centers, Adv. Phys. **47**, 599 (1998).

[8] I. Affleck and A. W. W. Ludwig, The Kondo Effect, conformal field theory and fusion rules, Nucl. Phys. B **352**, 849 (1991).

[9] M. Jarrell, H. Pang, D. L. Cox, and K. H. Luk, Two-Channel Kondo Lattice: An Incoherent Metal, Phys. Rev. Lett. **77**, 1612 (1996).

[10] A. Tsuruta, A. Kobayashi, Y. Ōno, T. Matsuura, and Y. Kuroda, Non-Fermi liquid in multichannel degenerate Anderson lattice, J. Phys. Soc. Jpn. **68**, 2491 (1999).

[11] A. Tsuruta and K. Miyake, Non-Fermi liquid and Fermi liquid in two-channel Anderson lattice model: Theory for PrA_2Al_{20} (A = V, Ti) and $PrIr_2Zn_{20}$, J. Phys. Soc. Jpn. **84**, 114714 (2015).

[12] S. Hoshino, J. Otsuki, and Y. Kuramoto, Diagonal Composite Order in a Two-Channel Kondo Lattice, Phys. Rev. Lett. **107**, 247202 (2011).

[13] S. Hoshino, J. Otsuki, and Y. Kuramoto, Resolution of entropy $\ln\sqrt{2}$ by ordering in two-channel Kondo lattice, J. Phys. Soc. Jpn. **82**, 044707 (2013).

[14] P. Chandra, P. Coleman, and R. Flint, Hastatic order in the heavy-fermion compound URu_2Si_2, Nature (London) **493**, 621 (2013).

[15] G. R. Stewart, Non-Fermi-liquid behavior in d- and f-electrons metals, Rev. Mod. Phys. **73**, 797 (2001).

[16] C. L. Seaman, M. B. Maple, B. W. Lee, S. Ghamaty, M. S. Torikachvili, J.-S. Kang, L. Z. Liu, J. W. Allen, and D. L. Cox, Evidence for Non-Fermi-Liquid Behavior in the Kondo Alloy $Y_{1-x}U_xPd_3$, Phys. Rev. Lett. **67**, 2882 (1991).

[17] K. A. McEwen, J.-G. Park, A. J. Gipson, and G. A. Gehring, A new model for the crystal field and the quadrupolar phase transitions of UPd_3, J. Phys.: Condens. Matter **15**, S1923 (2003).

[18] M. McElfresh, M. B. Maple, J. O. Willis, D. Schiferl, J. L. Smith, Z. Fisk, and D. L. Cox, Pressure dependence of the static magnetic susceptibility of the heavy-fermion superconductor UBe_{13}, Phys. Rev. B **48**, 10395 (1993).

[19] F. G. Aliev, S. Vieira, R. Villar, H. P. van der Meulen, K. Bakker, and A. V. Andreev, Anomalous ground state of $U_{0.9}Th_{0.1}Be_{13}$, JETP Lett. **58**, 762 (1993).

[20] H. Amitsuka and T. Sakakibara, Single uranium-site properties of the dilute heavy electron system $U_xTh_{1-x}Ru_2Si_2$ ($x \leqslant 0.07$), J. Phys. Soc. Jpn. **63**, 736 (1994).

[21] T. Kawae, K. Kinoshita, Y. Nakaie, N. Tateiwa, K. Takeda, H. S. Suzuki, and T. Kitai, Possible Observation of the Quadrupolar Kondo Effect in Dilute Quadrupolar System $Pr_xLa_{1-x}Pb_3$ for $x \leqslant 0.05$, Phys. Rev. Lett. **96**, 027210 (2006).

[22] T. Nasch, W. Jeitschko, and U. C. Rodewald, Ternary rare earth transition metal zinc compounds RT_2Zn_{20} with T = Fe, Ru, Co, Rh, and Ni, Z. Naturforsch., B **52**, 1023 (1997).

[23] T. Onimaru, K. T. Matsumoto, Y. F. Inoue, K. Umeo, T. Sakakibara, Y. Karaki, M. Kubota, and T. Takabatake, Antiferroquadrupolar Ordering in a Pr- Based Superconductor $PrIr_2Zn_{20}$, Phys. Rev. Lett. **106**, 177001 (2011).

[24] A. Sakai and S. Nakatsuji, Kondo effects and multipolar order in the cubic $PrTr_2Al_{20}$ (Tr = Ti, V), J. Phys. Soc. Jpn. **80**, 063701 (2011).

[25] T. J. Sato, S. Ibuka, Y. Nambu, T. Yamazaki, T. Hong, A. Sakai, and S. Nakatsuji, Ferroquadrupolar ordering in $PrTi_2Al_{20}$, Phys. Rev. B **86**, 184419 (2012).

[26] K. Iwasa, H. Kobayashi, T. Onimaru, K. T. Matsumoto, N. Nagasawa, T. Takabatake, S. Ohira-Kawamura, T. Kikuchi, Y. Inamura, and K. Nakajima, Well-defined crystal field splitting schemes and non-Kramers doublet ground states of f electrons in PrT_2Zn_{20} (T = Ir, Rh, and Ru), J. Phys. Soc. Jpn. **82**, 043707 (2013).

[27] D. Yazici, T. Yanagisawa, B. D. White, and M. B. Maple, Nonmagnetic ground state in the cubic compounds $PrNi_2Cd_{20}$ and $PrPd_2Cd_{20}$, Phys. Rev. B **91**, 115136 (2015).

[28] I. Ishii, H. Muneshige, Y. Suetomi, T. K. Fujita, T. Onimaru, K. T. Matsumoto, T. Takabatake, K. Araki, M. Akatsu, Y. Nemoto, T. Goto, and T. Suzuki, Antiferro-quadrupolar ordering at the lowest temperature and anisotropic magnetic field-temperature phase diagram in the cage compound $PrIr_2Zn_{20}$, J. Phys. Soc. Jpn. **80**, 093601 (2011).

[29] W. Higemoto, T. U. Ito, K. Ninomiya, T. Onimaru, K. T. Matsumoto, and T. Takabatake, Multipole and superconducting state in $PrIr_2Zn_{20}$ probed by muon spin relaxation, Phys. Rev. B **85**, 235152 (2012).

[30] T. Onimaru, K. T. Matsumoto, Y. F. Inoue, K. Umeo, Y. Saiga, Y. Matsushita, R. Tamura, K. Nishimoto, I. Ishii, T. Suzuki, and T. Takabatake, Superconductivity and structural phase transitions in caged compounds RT_2Zn_{20} (R = La, Pr, T = Ru, Ir), J. Phys. Soc. Jpn. **79**, 033704 (2010).

[31] T. Onimaru, N. Nagasawa, K. T. Matsumoto, K. Wakiya, K. Umeo, S. Kittaka, T. Sakakibara, Y. Matsushita, and T. Takabatake, Simultaneous superconducting and antiferro-quadrupolar transitions in $PrRh_2Zn_{20}$, Phys. Rev. B **86**, 184426 (2012).

[32] A. Sakai, K. Kuga, and S. Nakatsuji, Superconductivity in the ferroquadrupolar state in the quadrupolar Kondo lattice $PrTi_2Al_{20}$, J. Phys. Soc. Jpn. **81**, 083702 (2012).

[33] M. Tsujimoto, Y. Matsumoto, T. Tomita, A. Sakai, and S. Nakatsuji, Heavy-Fermion Superconductivity in the Quadrupole Ordered State of PrV_2Al_{20}, Phys. Rev. Lett. **113**, 267001 (2014).

[34] K. Matsubayashi, T. Tanaka, A. Sakai, S. Nakatsuji, Y. Kubo, and Y. Uwatoko, Pressure-Induced Heavy Fermion Superconductivity in the Nonmagnetic Quadrupolar System $PrTi_2Al_{20}$, Phys. Rev. Lett. **109**, 187004 (2012).

[35] Y. Tokunaga, H. Sakai, S. Kambe, A. Sakai, S. Nakatsuji, and H. Harima, Magnetic excitations and c-f hybridization effect in $PrTi_2Al_{20}$ and PrV_2Al_{20}, Phys. Rev. B **88**, 085124 (2013).

[36] M. Matsunami, M. Taguchi, A. Chainani, R. Eguchi, M. Oura, A. Sakai, S. Nakatsuji, and S. Shin, Kondo resonance in $PrTi_2Al_{20}$: Photoemission spectroscopy and single-impurity Anderson model calculations, Phys. Rev. B **84**, 193101 (2011).

[37] Y. Machida, T. Yoshida, T. Ikeura, K. Izawa, A. Nakama, R. Higashinaka, Y. Aoki, H. Sato, A. Sakai, S. Nakatsuji, N. Nagasawa, K. Matsumoto, T. Onimaru, and T. Takabatake, Anomalous enhancement of Seebeck coefficient in Pr-based 1-2-20 system with non-Kramers doublet ground states, J. Phys.: Conf. Ser. **592**, 012025 (2015).

[38] M. Matsushita, J. Sakaguchi, Y. Taga, M. Ohya, S. Yoshiuchi, H. Ota, Y. Hirose, K. Enoki, F. Honda, K. Sugiyama, M. Hagiwara, K. Kindo, T. Tanaka, Y. Kubo, T. Takeuchi, R. Settai, and Y. Ōnuki, Fermi surface property and characteristic crystalline electric field effect in $PrIr_2Zn_{20}$, J. Phys. Soc. Jpn. **80**, 074605 (2011).

[39] Y. Shimura, M. Tsujimoto, B. Zeng, L. Balicas, A. Sakai, and S. Nakatsuji, Field-induced quadrupolar quantum criticality in PrV_2Al_{20}, Phys. Rev. B **91**, 241102(R) (2015).

[40] K. Hattori and H. Tsunetsugu, Antiferro quadrupole orders in non-Kramers doublet systems, J. Phys. Soc. Jpn. **83**, 034709 (2014).

[41] T. Sakakibara, H. Mitamura, T. Tayama, and H. Amitsuka, Faraday force magnetometer for high-sensitivity magnetization measurements at very low temperatures and high fields, Jpn. J. Appl. Phys. **33**, 5067 (1994).

[42] J. Kondo, Internal magnetic field in rare earth metals, J. Phys. Soc. Jpn. **16**, 1690 (1961).

[43] T. Dahm and K. Ueda, NMR Relaxation and Resistivity from Rattling Phonons in Pyrochlore Superconductors, Phys. Rev. Lett. **99**, 187003 (2007).

[44] T. Hasegawa, N. Ogita, and M. Udagawa, First-principles calculations of lattice vibrations on LaT_2Zn_{20} (T = Ru and Ir), J. Phys.: Conf. Ser. **391**, 012016 (2012).

[45] K. Wakiya, T. Onimaru, S. Tsutsui, K. T. Matsumoto, N. Nagasawa, A. Q. R. Baron, T. Hasegawa, N. Ogita, M. Udagawa, and T. Takabatake, Interplay between low-energy optical phonon modes and structural transition in PrT_2Zn_{20} (T = Ru and Ir), J. Phys.: Conf. Ser. **592**, 012024 (2015).

[46] K. Wakiya, T. Onimaru, S. Tsutsui, T. Hasegawa, K. T. Matsumoto, N. Nagasawa, A. Q. R. Baron, N. Ogita, M. Udagawa, and T. Takabatake, Low-energy optical phonon modes in the caged compound $LaRu_2Zn_{20}$, Phys. Rev. B **93**, 064105 (2016).

[47] T. Ikeura, T. Matsubara, Y. Machida, K. Izawa, N. Nagasawa, K. T. Matsumoto, T. Onimaru, and T. Takabatake, Anomalous enhancement of Seebeck coefficient in $PrIr_2Zn_{20}$, JPS Conf. Proc. **3**, 011091 (2014).

[48] S. Yotsuhashi and H. Maebashi, Crossover temperature from non-Fermi liquid to Fermi liquid behavior in two types of impurity Kondo model, J. Phys. Soc. Jpn. **71**, 1705 (2002).

[49] H. Kusunose and T. Onimaru, Competition between quadrupole and magnetic Kondo effects in non-Kramers doublet systems, J. Phys.: Conf. Ser. **592**, 012099 (2015).